Creating Opal–Templated Continuous Conducting Polymer Films with Ultralow Percolation Thresholds Using Thermally Stable Nanoparticles

7 AUTHORS, INCLUDING:

Dong Jin Kang
Korea Advanced Institute of Science and Tec…

30 PUBLICATIONS   **356** CITATIONS

SEE PROFILE

Minsoo P. Kim
New York University

12 PUBLICATIONS   **145** CITATIONS

SEE PROFILE

Hyunjung Jung
Korea University

17 PUBLICATIONS   **166** CITATIONS

SEE PROFILE

Joona Bang
Korea University

105 PUBLICATIONS   **2,496** CITATIONS

SEE PROFILE

Creating Opal-Templated Continuous Conducting Polymer Films with Ultralow Percolation Thresholds Using Thermally Stable Nanoparticles

Dong Jin Kang,[†] Taegyun Kwon,[†] Minsoo P. Kim,[†] Chul-Hee Cho,[†] Hyunjung Jung,[‡] Joona Bang,[‡] and Bumjoon J. Kim[†,*]

[†]Department of Chemical and Biomolecular Engineering, Korea Advanced Institute of Science and Technology (KAIST), Daejeon 305-701, Republic of Korea and [‡]Department of Chemical and Biological Engineering, Korea University, Seoul 136-701, Republic of Korea

Continuous polymer blends based on high internal polymeric phase emulsions (HIPPEs) have attracted a great deal of attention in various fields such as membranes, foams, and barriers. In particular, continuous conducting polymer films are of great importance for their application in optoelectronic devices, including polymer solar cells and LEDs.[1−5] However, conducting polymers usually suffer from their low processability, low mechanical strength, and (importantly) high cost. For applications requiring both conductivity and good mechanical strength such as organic electronics and coatings, one good approach involves blending the conducting polymer with a low-cost polymer matrix that provides the desired mechanical properties without interfering with the conducting polymer's unique features such as electrical and optical properties.[6−9] However, simple blending usually does not allow the degree of morphological control that ensures a conducting polymer has continuous phases, because the entropy of mixing is generally low for polymers; that is, solid polymer blends tend to be phase-separated at the macroscopic scale. Therefore, a high concentration of the minor component is required to produce a continuous percolated structure in binary polymer blends.[10] The decrease in the percolation threshold of one component to achieve continuity at low concentrations would be an important achievement in creating continuous films for optoelectronic applications. As an example, Qiu et al.[11] showed that the percolation threshold of conducting poly(3-hexylthiophene) (P3HT) polymers in an insulating polystyrene (PS) matrix can be dramatically

ABSTRACT We propose a novel and robust strategy for creating continuous conducting polymer films with ultralow percolation thresholds using polymer-coated gold nanoparticles (Au NPs) as surfactant. Continuous poly(triphenylamine) (PTPA) films of high internal phase polymeric emulsions were fabricated using an assembly of cross-linked polystyrene (PS) colloidal particles as template. Polymer-coated Au NPs were designed to be thermally stable even above 200 °C and neutral to both the PS and PTPA phases. Therefore, the Au NPs localize at the PS/PTPA interface and function as surfactant to efficiently produce a continuous conducting PTPA polymer film with very low percolation thresholds. The volume fraction threshold for percolation of the PTPA phase with insulating PS colloids (as measured by electron microscopy and conductivity measurements) was found to be 0.20. In contrast, with the addition of an extremely low volume fraction (ϕ_p = 0.35 vol %) of surfactant Au NPs, the volume fraction threshold for percolation of the PTPA phase was dramatically reduced to 0.05. The SEM and TEM measurements clearly demonstrated the formation of a continuous PTPA phase within the polyhedral phase of PS colloids. To elucidate the influence of the nanoparticle surfactant on the blend films, the morphology and conductivity of the blends at different PS colloid/PTPA volume ratios were carefully characterized as a function of the Au NP concentration. Our approach provides a methodology for a variety of applications that require a continuous phase for the transport of molecular species, ions, or electrons at low concentrations and a second phase for mechanical support or the conduction of a separate species.

KEYWORDS: polymer-coated nanoparticles · conducting polymer · conducting film · compatibilizer · self-assembled colloids

reduced by using a proper solvent that helps the formation of crystalline P3HT nanowires. Another interesting way to achieve low percolation threshold materials is a templating approach with surfactants. This approach could be more generally applicable, because it does not require a strong crystalline component in the blend. Recently, the fabrication of a continuous conducting phase with insulating polymer blends using block copolymer surfactants has been reported.[10,12,13] For example, Mezzenga et al.[14] suggested that a continuous conducting polymer phase could be formed by a

templating approach that allows the synthesis of HIPPE structures. Using block copolymer surfactants, HIPPE structures were produced in which a continuous minority phase is present in a volume fraction as low as 0.13. This technique was found to be highly desirable for producing blends with unique electrical and barrier properties from the minority low percolating phase.

Block and graft copolymers have been widely used as compatibilizers for the fabrication of continuous morphologies within polymer blends.[15−24] The removal of these surfactants is very important for many applications because they have been shown to affect the properties of the resulting polymer; however, the surfactants are difficult and costly to remove.[25] Moreover, these copolymer stabilizers often form micelles within one of the blended materials, and thus the use of premade copolymers is impractical, whereas the *in situ* formation of copolymers by reactive blending typically requires suitably functionalized precursor polymers.[22,26,27] On the other hand, nanoparticles (NPs) can act as surfactant molecules, when they are adsorbed onto an immiscible polymer−polymer interface. Such "particle surfactants" can be active or passive in conferring special properties to the composition, and they have been demonstrated to help create emulsions by decreasing the interfacial tension and stabilizing the film between droplets, thus preventing coalescence.[28−31] Surfactant-free Pickering emulsions stabilized using titania and silica NPs whose surfaces are modified with oleic acid have also been reported.[32−35] Furthermore, in comparison with conventional emulsions that are stabilized by surfactants, particle-stabilized emulsions are extremely stable because of the quasi-irreversible adsorption of particles to the interface.

Particles must be positioned precisely at the interface between two different polymers to achieve surfactant-like properties, and a recent strategy to control the location of NPs in a block copolymer or polymer blend involves tuning the surface properties of NPs by end-attaching ligands, such as organic small molecules,[36−40] homopolymers,[34,41−45] mixtures of homopolymers,[46,47] or copolymers,[48,49] to their surface. It should be noted that the adsorption energy of NPs onto the interface, which determines the ability of the NPs to serve as a surfactant, is strongly dependent on the enthalpic interaction between the NP surface and the polymer matrix. Recently, the use of polymer-coated NPs as stabilizers in polymer and/or fluid mixtures has been demonstrated.[29,34,50−52] For example, our previous work showed that Au NPs at the interface between poly(styrene-*b*-2-vinylpyridine) (PS-*b*-P2VP) block copolymers were able to act as surfactants and induce the formation of a uniform bicontinuous structure with characteristic dimensions of less than 100 nm.[53,54]

In the present work, we developed a template approach to fabricate a continuous HIPPE of a conducting polymer film based on colloidal particles with a narrow size distribution combined with a polymer-coated Au NP surfactant. First, we designed thermally stable Au NPs coated with properly designed polymeric ligands that neutrally interact with the PS colloids and poly(triphenylamine) (PTPA) matrix. Whereas the PS colloids provide an insulating template that supports the PTPA phase, the PTPA polymers retain high hole conductivity and have been successfully applied to electronic applications, particularly in organic light-emitting diodes. The Au NP surfactant can be used to pack colloidal systems and to maintain a dispersed colloidal phase embedded in a continuous percolating phase. For example, the volume fraction threshold for percolation of the PTPA phase with insulating PS colloids, as measured by electron microscopy and conductivity measurements, was 0.20. In contrast, the volume fraction threshold for percolation of the PTPA phase was dramatically reduced to 0.05 with an addition of the extremely low volume fraction of Au NP surfactant of 0.0035. Furthermore, we have assessed the effects of nanoparticle surfactants on the blend morphology and properties by measuring the conductivity of the blends at different PS colloid/PTPA volume ratios and surfactant volume fractions. Our approach provides a general platform for building continuous polymer films with a very low percolation threshold.

RESULTS AND DISCUSSION

To create the continuous phase in the immiscible polymer blends at low percolation threshold, we have applied a template approach combined with the surfactants to enhance the miscibility between two different polymer domains. The conventional surfactants to reduce the interfacial tension are polymeric ones such as block or graft copolymers. However, a significant amount of the polymer surfactants are typically present as micelles and/or free chains within a homopolymer domain. As an alternative means, nanoparticles could act as effective compatibilizers because they can be irreversibly adsorbed to the interface between the polymer domains due to their high adsorption energy.[28,55] In addition, they can occupy a large interfacial area at a given volume fraction. For these reasons, we have decided to use Au NP surfactants. Moreover, the trace of Au NPs within the polymer matrix can be readily detected by electron microscopy due to higher electron density; thereby the correlation between NP behaviors and resulting material property can be easily monitored. In this case, there are two critical requirements for Au NPs in their use as compatibilizers in the PS colloid/PTPA polymer system to create a continuous conducting polymer film with low threshold. First, because polymers often have high glass transition temperatures (T_g) (*i.e.*, PS $T_g \approx 100$ °C, PTPA $T_g \approx 140$ °C), the polymer-coated Au NPs should possess excellent thermal stability under their thermal
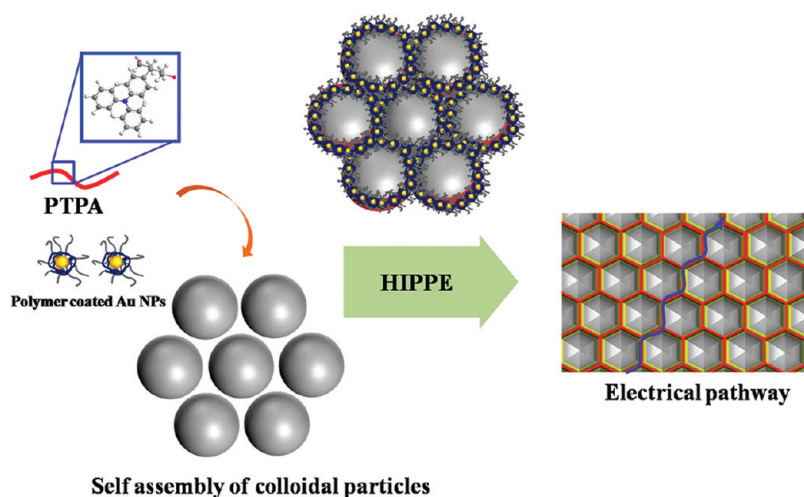
Scheme 1. Schematic illustration of our experimental approach to create a continuous conducting polymer film using PS colloidal template and nanoparticle surfactant.
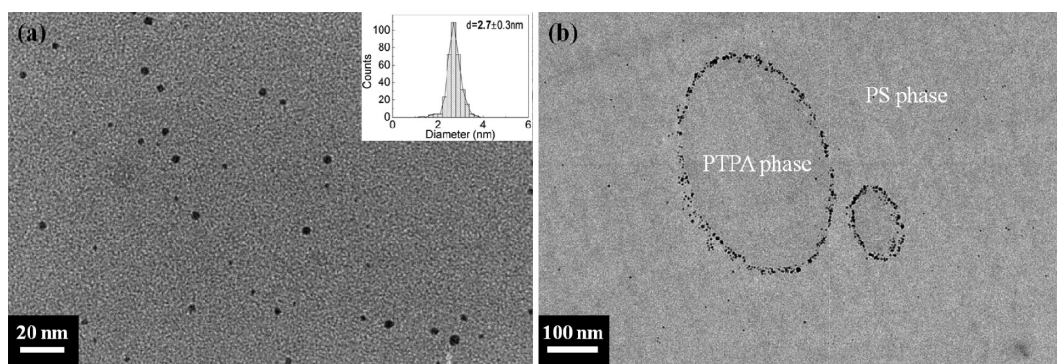

Figure 1. (a) TEM image of P(S-*b*-SN$_3$)-Au NPs and corresponding histogram (inset) of their size distribution; P(S-*b*-SN$_3$)-Au NPs have a core diameter of 2.72 ± 0.31 nm. (b) TEM morphology of PS and PTPA homopolymer blends with the addition of 1 vol % P(S-*b*-SN$_3$)-Au NPs after annealing for 48 h at 200 °C. Most of the Au NPs were segregated at the PS/PTPA interface of the blends without any aggregation.

processing window with the polymer blend. Second, the Au NPs should be located at the interface between the domains of two different polymers for their use as compatibilizers.

To meet these requirements, we designed thermally stable Au NPs coated with properly designed polymers that neutrally interact with PS and PTPA matrixes. A low molecular weight thiol-terminated P(S-*b*-SN$_3$) block copolymer (P(S-*b*-SN$_3$)-SH) was synthesized by reversible addition fragmentation chain transfer (RAFT) polymerization to produce a total molecular weight (M_n) of ~2400 g/mol and a polydispersity index (PDI) of 1.12, where the M_n of the PS and PSN$_3$ blocks were 1.9 and 0.5 kg/mol, respectively. According to previous studies,[44,47] the low M_n of thiol-terminated polymers allows a large number of polymer chains to be grafted to the gold surface. P(S-*b*-SN$_3$)-SH coated Au NPs (P(S-*b*-SN$_3$)-Au NPs) were synthesized by the two-phase method. The diameter of the Au core measured by TEM was 2.72 nm, as shown in Figure 1a. The parameter Σ, which is the areal chain density of the P(S-*b*-SN$_3$) chains on the Au NPs, is important in determining the

enthalpic interaction between the polymer-coated NPs and the polymer matrix. The Σ of the P(S-*b*-SN$_3$)-Au NPs was estimated to be 1.07 chains/nm^2, which is not high enough to completely cover the Au NPs surface.[47] The thermal stability of the P(S-*b*-SN$_3$)-Au NPs was evaluated by two different methods in both the solvent and the thin film as similar to that reported in our previous work (Figure S1).[52] The diameters of the Au NPs remained unchanged after annealing at 220 °C for 48 h, indicating that the P(S-*b*-SN$_3$)-Au NPs are thermally stable and can be used in high-temperature processes, unlike traditional polymer-coated Au NPs, which do not have cross-linked shells. The resulting Au NPs consist of nonpolar PS outer brushes and a polar PSN$_3$ inner cross-linked shell. Therefore, it can be anticipated that the PS outer shell is compatible with the PS matrix, while the more polar PSN$_3$ inner shell and bare Au NP surface can favorably interact with the polar PTPA matrix due to the existence of nitrogen in PTPA.

To test whether P(S-*b*-SN$_3$)-Au NPs can be used as compatibilizers in PS/PTPA blends, we prepared the nanocomposite sample containing PS and PTPA with a 1.0

vol % of P(S-b-SN$_3$)-Au NPs, as shown by cross-sectional TEM images in Figure 1b. To prepare the nanocomposite samples, a 2 wt % solution of a blend of PS/PTPA (80:20 v/v) in dichloromethane was mixed with the Au NPs to produce a particle volume fraction (ϕ_p) of 1 vol %. The M_n and PDI for the PS were 47 kg/mol and 1.13, respectively. The films cast from the solutions were annealed at 220 °C for 48 h and microtomed to examine their morphology by TEM. Because of the immiscibility between PS and PTPA, the morphology of the polymer blends displays two distinct domains; that is, droplets of one polymer domain are dispersed within a matrix of the other polymer. When the P(S-b-SN$_3$)-Au NPs were mixed with the PS/PTPA blend, a dramatic degree of localization of the Au NPs was observed at the polymer/polymer interface. This phenomenon can be explained by a balanced interaction between P(S-b-SN$_3$)-Au NPs and PS/PTPA matrix, as mentioned above. Furthermore, the Σ of the P(S-b-SN$_3$) chains on the Au NPs is lower than the critical Σ value required to fully cover the bare Au surface and the inner PSN$_3$ shell.[49,56] Therefore, the P(S-b-SN$_3$)-Au NPs are nonselective to either the PS or PTPA phase. Instead, the NPs localize at the interface in order to reduce the interfacial tension between PS and PTPA phases and to avoid the entropic penalty from polymer matrix chains if the NPs are dispersed in either the PS or PTPA domains. These results indicate that the thermally stable Au NPs can function as compatibilizers in the PS/PTPA blends.

On the basis of the results of the P(S-b-SN$_3$)-Au NPs with PS/PTPA blend system shown in Figure 1, a continuous PTPA conducting polymer phase in a PS colloidal system was prepared using the P(S-b-SN$_3$)-Au NPs as surfactants. Cross-linked PS colloidal particles were used as a template to produce the continuous PTPA phase. A 1 wt % THF solution of PS colloid and PTPA with 0.35 vol % Au NPs was spin coated onto the silicon substrates to result in the nanocomposite films with a monolayer of PS colloids. Figure 2 represents the morphological behavior of the PS colloid/PTPA blends with and without P(S-b-SN$_3$)-Au NPs as characterized by FE-SEM, confocal microscopy, and TEM measurements. Figure 2a and b, respectively, represent SEM images of PS colloid/PTPA blends (95:5 v/v) without and with a very low volume fraction of Au NP surfactant (ϕ_p = 0.35%). Two notable features should be mentioned in Figure 2b. First, compared with the disordered structure of PS colloids in nonannealed blend films (see Figure S3), it is clear that the colloidal particles undergo strong rearrangement upon annealing, deforming to polyhedrons wetted by a low volume fraction of the PTPA phase. During annealing, driven by the surface tension associated with trapped voids in the dried dispersion and the high chemical potential of the surfactant NPs in the medium surrounding the colloids, the morphology of the system reorganizes, and
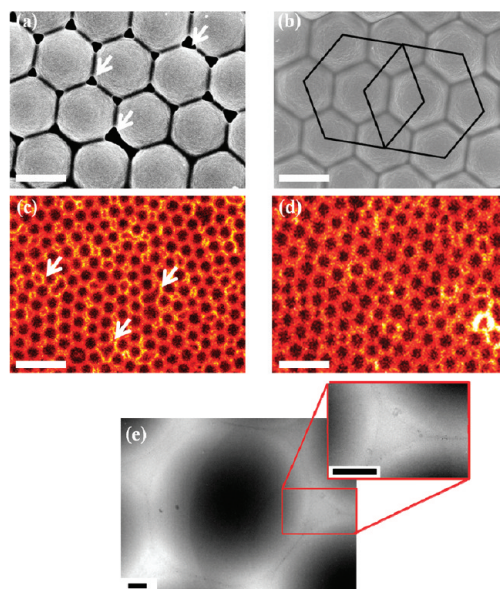
Figure 2. Morphological behavior of PS colloid/PTPA blends with and without P(S-b-SN$_3$)-Au NP surfactant. SEM images of PS colloid/PTPA blends (95:5 v/v) (a) without and (b) with Au NPs (ϕ_p = 0.35%). The scale bar is 3 μm. Confocal laser scanning microscopy (CLSM) images show PS colloid/PTPA blends (95:5 v/v) (c) without and (d) with Au NPs (ϕ_p = 0.35%). The scale bar is 10 μm. Because the PTPA phase is doped with red-colored Nile-Red dye, the red phase is the PTPA phase. (e) TEM image showing the complete infiltration of the PTPA phase in the PS colloid/PTPA blend with 0.35 vol % Au NPs, revealing that most of the Au NPs clearly segregate along the PS/PTPA interface. The scale bar is 500 nm.

the lightly cross-linked colloids deform to polyhedrons to minimize their free energy. Second, this morphology shows complete infiltration of the PTPA phase surrounding the PS colloids, in contrast to that of the PS colloid/PTPA blend without the Au NP surfactant. Without the P(S-b-SN$_3$)-Au NPs in the blend in Figure 2a, the free surface of the PS colloids can be only partially wetted by the PTPA phase, leaving empty space in between as indicated by the white arrows. This is due to the low compatibility between the PS colloids and the PTPA phase at the interface.

To confirm the successful infiltration of PTPA into the empty spaces of the self-assembled PS colloidal particles and to identify their continuous pathway, the PS colloid/PTPA phases with and without the Au NP surfactant were examined by confocal laser scanning microscopy (CLSM). All samples were prepared in the same conditions that were previously used for the SEM measurements except for the addition of red-emitting Nile-Red dye molecules to produce contrast in the PTPA phase. Because the PS colloids were already cross-linked, the PTPA phase was selectively doped with Nile-Red, resulting in the red color in the CLSM image. Fluorescence intensity was measured using an excitation wavelength of 530 nm and an emission wavelength of 640 nm. Figure 2c and d show CLSM images of the PS/PTPA blend without and with the Au
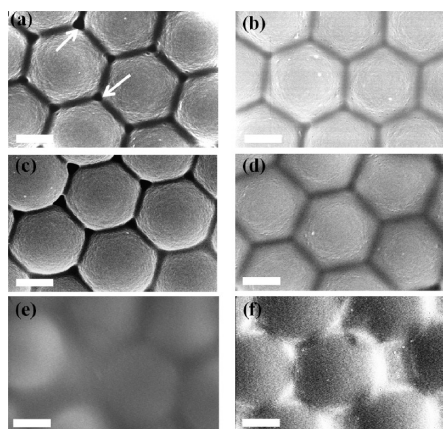
Figure 3. SEM images of PS colloid particle/PTPA morphology at various PTPA volume fractions ranging from 95:5 (v/v) to 80:20 (v/v). PS colloid/PTPA blends with volume fraction ratios of (a) 95:5, (c) 90:10, and (e) 80:20. PS colloid/PTPA blends with surfactant Au NPs (ϕ_p = 0.35%) and PS/PTPA volume fraction ratios of (b) 95:5, (d) 90:10, and (f) 80:20. The scale bar is 1.5 μm.

NP surfactant, respectively. The effect of Au NPs in PS colloid/PTPA films shown in Figure 2a and b clearly confirmed that the PS colloids self-organized into hexagonally ordered microstructures embedded in the continuous PTPA phase with Au NPs as shown in Figure 2d. In contrast, without Au NP surfactant, large voids were present due to a lack of PTPA polymer infiltration between the PS colloids. This difference is driven by the large interfacial adsorption energy of the Au NPs to the PS colloid/PTPA interface and their high chemical potential in the medium surrounding the colloids. The Au NPs were redistributed and segregated to the interfaces of the colloidal particles during annealing. Evidence for the interfacial segregation of the Au NPs is provided by the TEM measurements in Figure 2e. A dark line of Au NPs along the interface between the PS colloids and the PTPA can be seen clearly, indicating that the interface between the assembled template and the continuous phase is stabilized with Au NPs acting as a surfactant.

The trend in the dramatic effect of polymer-coated Au NP surfactants on the blend morphology was also observed for other PS colloids/PTPA films with various PS/PTPA volume ratios. Figure 3 shows representative SEM images showing the morphology of various PS colloid particle/PTPA blends with PTPA volume fractions ranging from 95:5 (v/v) to 80:20 (v/v) without and with P(S-b-SN₃)-Au NPs as compatibilizer. The morphologies of the PS colloid particle/PTPA blends without Au NPs are shown in Figure 3a, c, and e. Void spaces are clearly visible between the PS colloids in the PS colloid/PTPA samples with low PTPA volume fractions of 0.05 and 0.10, indicating that the PTPA phase is not continuous. In contrast, with the addition of a very low volume fraction of Au NPs (ϕ_p = 0.35%), the empty spaces between the PS colloids disappeared

completely, showing the formation of a continuous PTPA phase. The interfacial energy between the PS colloidal particles and the PTPA phase was dramatically reduced by the addition of Au NPs, and the low volume fraction of PTPA polymers can provide a continuous phase as shown in Figure 3b and d. Simultaneously, the lightly cross-linked PS colloidal particles deformed into a hexagonal structure to eliminate the remaining voids. Similar phenomena of colloidal particle deformation in polymer blends have been reported by other researchers.[57−59] For example, Mezzenga et al.[57,59] reported the deformation of colloidal systems driven by PS-b-P2VP block copolymers that compatibilize PS colloids and the P2VP phase. On the other hand, at PTPA volume fractions above 0.2, the PTPA phase in a PS colloid/PTPA blend, even without Au NPs, can surround the PS colloids well, resulting in a continuous conducting phase in the colloidal system, as shown in Figure 3e.

To optimize the effects of the Au NP compatibilizer on the film morphology and electrical properties of the PS colloidal particle/PTPA blend, the morphology of the blend was investigated as a function of ϕ_p. Figure 4a−c present FE-SEM and TEM micrographs showing the morphology of a PS colloid/PTPA blend (95:5 v/v) at various ϕ_p: (a) 0.35%, (b) 1.0%, and (c) 1.5%. At this range of ϕ_p, all the PS colloidal particles were deformed into a closely packed polyhedral structure with a well-infiltrated PTPA phase. The TEM images clearly revealed that most of the Au NPs were localized along the PS/PTPA interface without aggregation, regardless of ϕ_p. Larger numbers of Au NPs were located at the interface at higher values of ϕ_p.

To demonstrate the importance of the compatibilizing effect of the Au NPs, the conductivities of PS colloid/PTPA blends with different ϕ_p values were carefully measured. Because each sample used for conductivity measurement covers a large area (1.8 cm × 1.3 cm) between the electrodes, a macroscopic view of the corresponding morphological change can be obtained by identifying correlations between the morphological and electrical properties of the blend samples. Figure 4d shows the conductivities of PS colloid/PTPA blends with the volume ratios of 95:5 and 90:10 at various ϕ values. First, it is remarkable that the addition of a small amount of Au NP surfactant (0.35 vol %) dramatically enhanced the conductivity of the PS colloid/PTPA blend. This result can be explained by the compatibilizing effect of Au NPs on the film morphology, as shown in Figure 3a and b. The continuous PTPA phase driven by the Au NP surfactant provides a pathway for electrical transport. This effect is much more pronounced with a PS colloid/PTPA film with a larger PTPA volume fraction (90:10), in which the conductivity was increased by 2 orders of magnitude by the addition of Au NPs. Interestingly, the conductivity became saturated with an increase of ϕ_p above
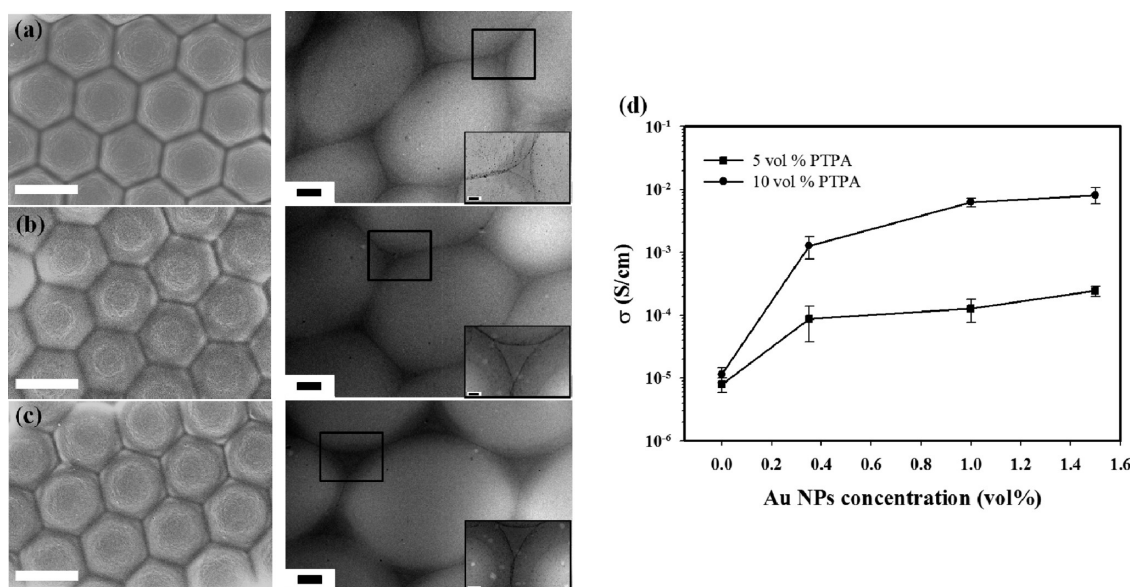
Figure 4. SEM (left column) and TEM (right column) images represent the morphology of a PS colloid/PTPA blend (95:5 v/v) at various Au NP concentrations. The PS colloid/PTPA blend with a ϕ_p of (a) 0.35%, (b) 1.0%, and (c) 1.5%. The scale bar is 3 μm for the SEM images and 500 nm for the TEM images. (d) Conductivity of the PS/PTPA blend for PS/PTPA volume ratios of 95:5 and 90:10 at various ϕ_p.

0.35%. This trend of conductivity at different ϕ_p values is consistent with that of the blend morphology as determined by SEM and TEM; there is almost no difference in the morphological aspects of PS colloid/PTPA blends at different ϕ_p values, as shown in Figure 4.

To gain deeper insight into the dependence of the morphological and electrical properties of the blend on ϕ_p, the coverage of the PS colloid/PTPA interface by the Au NPs was calculated as a function of ϕ_p. The particle volume fraction required to fully coat the PS colloids/PTPA interface was estimated with the following assumptions:[60] (1) all the particles are located at the interface, (2) the Au NPs and PS colloids are all monodispersed, and (3) the Au NPs form 2D squares laterally packed on the surfaces of the PS colloid droplets. The coverage by the P(S-b-SN₃)-Au NPs can be estimated from the ratio of the effective total surface area occupied by the Au NPs to the total surface area of the PS colloids, as in the following equation:

$$\text{Coverage} = \frac{A_{AuNP}}{A_{PS}} = \frac{\pi(R_{AuNP})^2 N_{AuNP}}{4\pi(R_{PS})^2 N_{PS}} \frac{1}{0.91} \quad (1)$$

where A_{AuNP} is the total effective area of the PS colloid surface covered by Au NPs; A_{PS} is the total surface area of the PS colloidal particles; R_{AuNP} (2.94 nm = (Au core radius + polymer shell thickness)) and R_{PS} (1.25 μm) are the radii of the Au NPs and PS colloidal particles, respectively; and N_{AuNP} and N_{PS} are the number of Au NPs and PS colloidal particles in a given volume of the sample. The factor 0.91 is the critical fraction of a two-dimensional close packing of circles. Considering all the experimental parameters at the PS colloid/PTPA volume ratio of 90:10, the particle volume fraction required to form a fully packed monolayer on the PS

colloid surface (ϕ_{pc}) was estimated to be 0.77 vol %. This means that the Au NPs at ϕ_p = 0.35% should cover a major part of the PS colloid surface (coverage = 0.45). The addition of particles at higher values of ϕ_p such as 1% or 1.5% should be more than enough to form a monolayer along the PS/PTPA interface. This estimate agrees well with our experimental results, as it clearly explains why the increase in conductivity by the addition of Au NPs became insignificant above ϕ_p = 0.35%, as shown in Figure 4b. Interestingly, the TEM images in Figure 4b and c reveal that at higher volume fractions (ϕ_p = 1% or 1.5%) almost no Au NPs are present in either the PS or PTPA domains; instead all the particles are localized along the PS colloid/PTPA interface in a thicker interfacial layer. The excess Au NPs at higher ϕ_p segregate to the PS colloid/PTPA interface but have minimal influence on the morphology or corresponding electrical properties of the blend.

It is worth noting that the Au NP surfactant provides thermal stability to the continuous PTPA phase in the blend film. All the samples containing Au NP surfactant that were used for morphological and electrical measurements were prepared by annealing at 170 °C for 8 h. However, identical SEM/TEM micrographs of the structure and identical conductivities were observed at longer annealing times (i.e., 48 h) and higher annealing temperatures (i.e., 200 °C). This finding indicates the high stability at this temperature range, which exists because the particles are irreversibly trapped at the interface between the polymer blends. The adsorption energy of the particles onto the interface between the PS and PTPA phases (E_a) can be expressed by the following equation:[46,61]

TABLE 1. Conductivities of PS Colloid/PTPA/Au NPs Blends As a Function of the PTPA Volume Fraction for ϕ_P = 0 and 1 vol %

	PTPA = 0.05 (S/cm)	PTPA = 0.10 (S/cm)	PTPA = 0.20 (S/cm)	PTPA = 0.30 (S/cm)
ϕ_p = 0 vol %	7.96×10^{-6}	1.15×10^{-5}	1.73×10^{-4}	2.31×10^{-2}
ϕ_p = 1 vol %	1.78×10^{-4}	1.28×10^{-3}	3.46×10^{-2}	6.46×10^{-2}

$$E_a/k_B T = (\pi R^2 \gamma_{PS-PTPA}/k_B T)(1 - |\cos(\theta)|)^2 \text{ where}$$

$$|\cos(\theta)| = \frac{|\gamma_{PS-NP} - \gamma_{PTPA-NP}|}{\gamma_{PS-PTPA}}$$

$$(2)$$

where R is the radius of the NP, and $\cos(\theta)$ is the ratio of the difference in interfacial tension between the NPs and the PS and PTPA blocks to that between the PS and the PTPA. For particles coated with P(S-b-SN$_3$)-Au NPs polymers that are compatible with PS and PTPA phases, respectively, $\cos(\theta) \ll 1$, and $E_a \approx \pi R^2 \gamma_{PS\text{-}PTPA}$ should be much higher than $k_B T$. Furthermore, because we expect that there is a strong favorable enthalpic interaction between the bare Au surface and nitrogen atoms in the PTPA polymer, E_a is expected to be even higher. In addition, any tendency of the P(S-b-SN$_3$)-Au NP polymers to segregate in 2D on the nanoparticle surfaces would further favor particle adsorption.[47,62,63] Therefore, we expect the particles to be strongly bound to the PS colloid/PTPA interface and to stabilize the blend morphology.

A deeper insight into the morphological transition caused by these surfactant Au NPs can be gleaned by examining the conductivity of the PS colloid/PTPA/Au NPs film as a function of volume fractions of PTPA and Au NPs. Figure 5 shows the conductivities of PS colloid/PTPA films with different PTPA volume fractions for ϕ_p values of 0% and 1%. All the conductivity values in Figure 5 were obtained from the films consisting of PTPA, Au NPs, and a monolayer of PS colloids, which were prepared under identical conditions for the previous morphological studies in Figure 3 and 4. It should also be mentioned that the hole conductivity of a pure PTPA film, without PS colloids, was measured as a control sample. The hole conductivity of the PTPA film (1.8 cm × 1.3 cm × 2.5 μm) was measured to be 2.03 S/cm, which agrees well with the previously reported value for hole conductivity of PTPA (~2.4 S/cm).[64] The conductivities of PS colloid/PTPA blends with various PTPA volume fractions were measured to find the percolation threshold for the PTPA volume fraction, which is directly related to the formation of a continuous PTPA phase in the blend. Below the PTPA volume fraction of 0.2, the conductivity remains very low ($<10^{-4}$ S/cm). On the other hand, the conductivity of the blend increases abruptly above a PTPA volume fraction of 0.2, indicating that the percolation volume
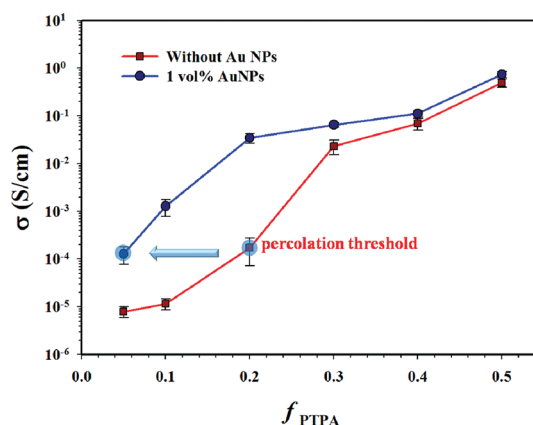

Figure 5. Conductivities of the PS colloid/PTPA film as a function of PTPA concentration without Au NPs and with Au NPs (ϕ_p = 1%).

fraction for the PTPA continuous phase is around 0.2. Interestingly, with the addition of Au NP surfactant (ϕ_p = 0.01), the volume fraction threshold for percolation of the PTPA phase was dramatically reduced to 0.05. In the presence of Au NP surfactant, the conductivity, even at the low PTPA volume fraction of 0.05, was measured at 1.78×10^{-4} S/cm, which is slightly higher than that of the PS/PTPA (80:20 v/v) blend without the Au NP surfactant (1.73×10^{-4} S/cm). In addition, it was clearly seen that the conductivity of PS/PTPA blends in the range from 95:5 to 80:20 was increased by 2 orders of magnitude by adding the Au NP surfactant. For example, the conductivity of the PS colloid/PTPA (80:20 v/v) blend was enhanced from 1.73×10^{-4} to 3.46×10^{-2} S/cm by the Au NP surfactant, which is almost a 200-fold increase. This increase in conductivity by the addition of a Au NP surfactant can be explained by the compatibilizing effect of the Au NPs on the blend morphology, thus promoting the formation of a continuous PTPA phase at a much lower PTPA volume fraction, as previously shown in Figure 4. The conductivity of the blend film shows results consistent with its morphological behavior since PTPA infiltrates into empty spaces between densely packed PS colloidal particles, creating a continuous phase that forms an electrical pathway. Above their percolation threshold (PTPA volume fraction = 0.2), the difference in conductivity between PS/PTPA blends with and without Au NP surfactants is less, because a continuous structure is also observed for PS/PTPA blends without Au NPs. The effect of the film thickness on the percolation threshold is under investigation, because the threshold for a continuous PTPA film in the PS colloid/PTPA blend could be dependent on the film thickness.

It should be emphasized that our system based on a polymer-coated Au NP surfactant has unique advantages. First, the surface properties of Au NPs can be easily controlled through the facile grafting of thiol end groups to obtain a surface with polymer ligands at a controlled areal density, which is a critical parameter

a

b
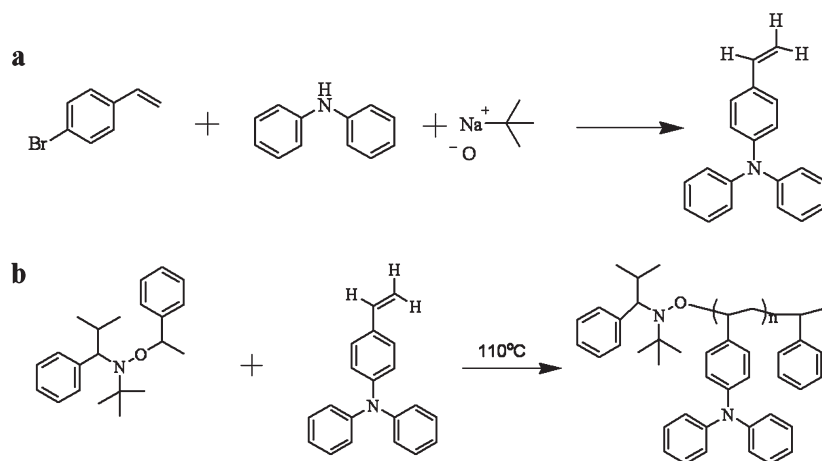
Scheme 2. Synthesis of TPA monomer and PTPA by NMP polymerization.

for producing NP surfactants for various polymer and/or fluid mixtures.[47,54] Second, the strong contrast between Au NPs and polymers under electron microscopy as well as their ability to absorb light in the visible regime make them well suited for model studies on the effect of nanoparticles in compatibilizing polymer blends. In addition, our Au NP surfactant has high thermal stability, which makes it perfectly suited for polymer blending that requires high-temperature processing. Furthermore, since Au NPs have extremely high conductivity, the electrical properties of the conducting polymer blends can be greatly enhanced if Au NPs are coated with properly chosen polymer ligands (*i.e.*, conducting polymers).

CONCLUSIONS

In this study, we successfully developed a simple and efficient route for fabricating continuous conducting polymer films with ultralow percolation thresholds. A conducting pathway through a minor continuous PTPA phase was successfully created based on an opal template of PS colloids and a thermally stable polymer-coated Au NP surfactant. P(S-*b*-SN$_3$)-Au NPs were designed to be thermally stable and to preferentially segregate at the PS colloid/PTPA interface. Thus, these Au NPs can function as compatibilizers for thermally processed PS colloid/PTPA blends. Au NPs surfactants were used to pack colloidal systems and to maintain a

dispersed colloidal phase embedded in a continuous percolating phase. TEM, SEM, and CLSM measurements revealed that the volume fraction threshold for percolation of the PTPA phase with insulating PS colloids was 0.20. In contrast, with the addition of an extremely small amount of Au NPs ($\phi_p = 0.35$ vol %), the volume fraction threshold for percolation of the PTPA phase was dramatically reduced to 0.05. The effect of the Au NP surfactant on the morphology of the PS colloid/PTPA film was further supported by conductivity measurements. The conductivity of PS colloid/PTPA blends ranging from 95:5 to 80:20 was dramatically increased by 2 to 3 orders of magnitude by the addition of Au NP surfactant. In addition, the continuous nature of the PTPA film caused by the Au NP surfactant was found to be very stable due to the strong adsorption energy of the Au NP compatibilizers onto the interface. Our findings demonstrate a new approach to fabricate a continuous conducting phase using a NP compatibilizer at very low volume fractions. Following our approach, new applications can be envisaged for semiconducting polymer blends that require only minimal concentrations of conducting polymers. Furthermore, the materials that can be fabricated using this method are potentially enhanced by the electrical, optical, magnetic, and/or catalytic properties of the inorganic nanoparticles that are incorporated into the continuous structure.

METHODS

Synthesis of 4-Vinyltriphenylamine. 4-Vinyltriphenylamine (VTPA) was synthesized as described in Scheme 2a. A mixture of 4-bromostyrene (1.83 g, 10.0 mmol), diphenylamine (3.38 g, 20.0 mmol), sodium *tert*-butoxide (1.92 g, 20.0 mmol), 3 mol % bis(dibenzylideneacetone)palladium (345 mg), and 6 mol % tri(*o*-tolyl)phosphine (182.62 mg) in anhydrous toluene (100 mL) was stirred at 110 °C for 2 h under a nitrogen atmosphere. Upon cooling to room temperature, the reaction mixture was extracted with EtOAc (300 mL). The separated organic layer was washed with water and brine, dried over MgSO$_4$, and concentrated *in vacuo*. The crude product was purified by column chromatography (CH$_2$Cl$_2$/*n*-hexanes = 1:10 v/v) as the eluant to

provide a white solid product (2.17 g, 80%): ^{1}H NMR (500 MHz, CDCl$_3$) δ 7.33–7.22 (m, 6H), 7.09 (d, $J = 7.6$ Hz, 4H), 7.06–7.00 (m, 4H), 6.67 (q, $J = 6.7$ Hz, 1H), 5.64 (d, $J = 17.1$ Hz, 1H), 5.15 (d, $J = 10.9$ Hz, 1H).

Synthesis of Poly(triphenylamine). Poly(triphenylamine) was synthesized by nitroxide-mediated radical polymerization (NMP) (Scheme 2b).[65] A mixture of VTPA (2.0 g, 7.37 mmol), NMP initiator (2.4 mg, 0.0074 mmol), and dimethylformamide (DMF) (10 mL) was added to a glass ampule. The mixture was degassed by freeze–pump–thaw, and the tube was sealed under vacuum. The mixture was allowed to react at 110 °C for 24 h. After precipitation in methanol (MeOH), the precipitate was collected by centrifugal sedimentation. The polymer was further purified

by dissolving in $CHCl_3$ and reprecipitating in MeOH several times. The product was collected by centrifugal sedimentation and dried under vacuum to form a white solid product (360 mg, 18%): ^{1}H NMR (500 MHz, $CDCl_3$) δ 6.95–6.54 (m, 14H $\times$ n), 1.99–1.49 (m, 3H $\times$ n). Anal. Calcd (%) for $(C_{20}H_{17}N)_n$: C, 88.52; H, 6.31; N, 5.16. Found: C, 88.31; H, 6.35; N, 5.34. The PTPA had a M_n of 25 kg/mol and a PDI of 1.18, which was measured by size exclusion chromatography (SEC).

Synthesis of Cross-Linked PS Colloidal Particles. Cross-linked PS colloidal particles were synthesized by dispersion polymerization.[66] Styrene monomer was purified with an aluminum oxide column. The other organic reagents were used without further purification, including divinylbenzene (DVB, 80%, mixture of isomers), MeOH, toluene, isopropyl alcohol (*i*-PrOH), poly(vinylpyrrolidone) (PVP, M_w = 55 000 g/mol), and 2,2-azobis(butyronitrile) (AIBN). In a 100 mL three-neck flask, PVP, styrene monomer (70% of the total amount), DVB, and dispersion medium (*i*-PrOH/toluene mixture, 95% of total amount) were introduced into the reaction vessel and heated to 70 °C. Nitrogen gas was bubbled through the solution for 1 h. The remaining styrene monomer (30%) with AIBN and the remaining dispersion medium (5%) were then added slowly to the reaction mixture. The reaction mixture was allowed to polymerize under a constant agitation rate and temperature. After polymerization, the PS colloidal particles were quenched by pouring the reaction mixture into MeOH at room temperature. The PS colloidal particles were isolated by filtration and washed several times with MeOH, MeOH/distilled water (50:50 v/v), and distilled water and finally dried at room temperature. The resulting PS colloidal particles had an average diameter of 2.5 μm. The cross-linked colloidal particles were observed to swell without dissolving in tetrahydrofuran (THF) for two weeks.

Synthesis of Thiol-Terminated Polystyrene-*b*-Poly(4-azidostyrene) Block Copolymers. Thiol-terminated P(S-*b*-SN$_3$) block copolymers were synthesized by RAFT polymerization using a dithioester RAFT agent and AIBN at 70 °C as reported in our previous studies.[52,67] First, the PS block was polymerized and then precipitated with cold MeOH. Then, 4-chlorostyrene monomer was added to the PS polymers to produce the second block of poly-(4-chlorostyrene). The polymer end group was converted to a thiol group by reaction with hexylamine, and an azide group was subsequently introduced by reacting with sodium azide. The total M_n and PDI of P(S-*b*-SN$_3$) were determined to be 2.4 kg/mol and 1.12, respectively, by SEC; the molecular weights of the PS and PSN$_3$ blocks were 1.9 and 0.5 kg/mol, respectively (Figure S2).

Synthesis of P(S-*b*-SN$_3$)-Coated Au NPs. The synthesis of P(S-*b*-SN$_3$)-Au NPs was performed using a two-phase system consisting of toluene and water with an initial mole feed ratio of P(S-*b*-SN$_3$) ligands to (Au atoms + P(S-*b*-SN$_3$) ligands) of 1:2.6.[44] The polymer ligands were carefully washed several times by centrifugation using the density-gradient method, in which the particles were washed through five different layers of dichloromethane and cyclohexane at various ratios with different densities.[68−70] The unwashed thiol-terminated polymer was monitored by SEC after each washing step. The areal chain density (Σ) and shell thickness of the polymers on the surface of the Au NPs were calculated to be 1.07 chain/nm^2 and 1.58 nm, respectively. These values are based on the Au core size, which was determined using TEM, and the relative weights of the Au core and the polymer ligands in the P(S-*b*-SN$_3$)-Au NPs, which was determined using thermogravimetric analysis.[44]

Device Fabrication and Measurement. Cross-linked PS colloidal particles and PTPA were chosen to produce continuous polymeric blends in which PTPA is maintained as a continuous phase. Blends of PS colloidal particles/PTPA/Au NPs were prepared with various volume fractions of PS colloids and P(S-*b*-SN$_3$)-Au NPs. Also, blends of PS colloidal particles/PTPA were prepared with various volume fractions of PTPA as control samples. The blend mixtures were sonicated for 1 h at room temperature and then stirred for another 1 h at 60 °C. The final mixtures were spuncast on Si substrate and NaCl substrate. The samples were annealed under vacuum at 170 °C for 1, 8, or 24 h and then for an additional 4 h at 80 °C. Thus prepared samples were further used for the characterization of morphological and electrical properties.

Field emission scanning electron microscopy (FE-SEM) and transmission electron microscopy (TEM) studies were performed to observe the morphology of the blend samples using a Hitachi S-4800 scanning electron microscope and a JEOL 2000FX, respectively. The continuous PTPA phases were observed through a confocal laser scanning microscope (Carl Zeiss, LSM 510) using Nile-Red dye molecules selectively doped into the PTPA phase of the blends. To assess conductivity, films of the PS colloids/PTPA/Au NP blends were prepared identically to those for the morphological study but on a glass substrate. Two parallel electrodes of carbon paste were applied using an adhesive mask. The measurements were performed using a two-probe method at room temperature, and the voltage was supplied by a Keithley 2400 source meter, ranging from −10 to 10 V across the sample. Conductivity was calculated taking into account the geometry of the samples.

Supporting Information Available: Additional GPC and SEM data. This material is available free of charge *via* the Internet at http://pubs.acs.org.

REFERENCES AND NOTES

1. Halls, J. J. M.; Walsh, C. A.; Greenham, N. C.; Marseglia, E. A.; Friend, R. H.; Moratti, S. C.; Holmes, A. B. Efficient Photodiodes from Interpenetrating Polymer Networks. *Nature* **1995**, *376*, 498–500.

2. Yu, G.; Gao, J.; Hummelen, J. C.; Wudl, F.; Heeger, A. J. Polymer Photovoltaic Cells: Enhanced Efficiencies via a Network of Internal Donor-Acceptor Heterojunctions. *Science* **1995**, *270*, 1789–1791.

3. Thompson, B. C.; Fréchet, J. M. J. Organic Photovoltaics - Polymer-Fullerene Composite Solar Cells. *Angew. Chem., Int. Ed.* **2008**, *47*, 58–77.

4. Peet, J.; Heeger, A. J.; Bazan, G. C. "Plastic" Solar Cells: Self-Assembly of Bulk Heterojunction Nanomaterials by Spontaneous Phase Separation. *Acc. Chem. Res.* **2009**, *42*, 1700–1708.

5. Cho, C. H.; Kang, H.; Kang, T. E.; Cho, H. H.; Yoon, S. C.; Jeon, M. K.; Kim, B. J. Controlling Side-Chain Density of Electron Donating Polymers for Improving Their Packing Structure and Photovoltaic Performance. *Chem. Commun.* **2011**, *47*, 3577–3579.

6. Wang, H. L.; Fernandez, J. E. Conducting Polymer Blends: Polypyrrole and Poly(vinyl methyl ketone). *Macromolecules* **1992**, *25*, 6179–6184.

7. Bernasik, A.; Wlodarczyk-Miskiewicz, J.; Luzny, W.; Kowalski, K.; Raczkowska, J.; Rysz, J.; Budkowski, A. Lamellar Structures Formed in Spin-Cast Blends of Insulating and Conducting Polymers. *Synth. Met.* **2004**, *144*, 253–257.

8. Kumar, A.; Baklar, M. A.; Scott, K.; Kreouzis, T.; Stingelin-Stutzmann, N. Efficient, Stable Bulk Charge Transport in Crystalline/Crystalline Semiconductor-Insulator Blends. *Adv. Mater.* **2009**, *21*, 4447–4451.

9. Lu, G. H.; Tang, H. W.; Huan, Y. A.; Li, S. J.; Li, L. G.; Wang, Y. Z.; Yang, X. N. Enhanced Charge Transportation in Semiconducting Polymer/Insulating Polymer Composites: The Role of an Interpenetrating Bulk Interface. *Adv. Funct. Mater.* **2010**, *20*, 1714–1720.

10. Kietzke, T.; Neher, D.; Landfester, K.; Montenegro, R.; Guntner, R.; Scherf, U. Novel Approaches to Polymer Blends Based on Polymer Nanoparticles. *Nat. Mater.* **2003**, *2*, 408–412.

11. Qiu, L. Z.; Lee, W. H.; Wang, X. H.; Kim, J. S.; Lim, J. A.; Kwak, D.; Lee, S.; Cho, K. Organic Thin-Film Transistors Based on Polythiophene Nanowires Embedded in Insulating Polymer. *Adv. Mater.* **2009**, *21*, 1349–1353.

12. Bose, S.; Bhattacharyya, A. R.; Kulkarni, A. R.; Pötschke, P. Electrical, Rheological and Morphological Studies in Co-continuous Blends of Polyamide 6 and Acrylonitrile-Butadiene-Styrene with Multiwall Carbon Nanotubes Prepared by Melt Blending. *Compos. Sci. Technol.* **2009**, *69*, 365–372.

13. Tran-Cong-Miyata, Q.; Nishigami, S.; Ito, T.; Komatsu, S.; Norisuye, T. Controlling the Morphology of Polymer Blends Using Periodic Irradiation. *Nat. Mater.* **2004**, *3*, 448–451.

14. Mezzenga, R.; Ruokolainen, J.; Fredrickson, G. H.; Kramer, E. J.; Moses, D.; Heeger, A. J.; Ikkala, O. Templating Organic Semiconductors *via* Self-Assembly of Polymer Colloids. *Science* **2003**, *299*, 1872–1874.

15. Noolandi, J.; Hong, K. M. Effect of Block Copolymers at a Demixed Homopolymer Interface. *Macromolecules* **1984**, *17*, 1531–1537.

16. Leibler, L. Emulsifying Effects of Block Copolymers in Incompatible Polymer Blends. *Macromol. Symp.* **1988**, *16*, 1–17.

17. Anastasiadis, S. H.; Gancarz, I.; Koberstein, J. T. Compatibilizing Effect of Block Copolymers Added to the Polymer/Polymer Interface. *Macromolecules* **1989**, *22*, 1449–1453.

18. Park, D. W.; Roe, R. J. Effect of Added Block Copolymer on the Phase-Separation Kinetics of a Polymer Blend. 2. Optical Microscopic Observations. *Macromolecules* **1991**, *24*, 5324–5329.

19. Semenov, A. N. Theory of Diblock-Copolymer Segregation to the Interface and Free Surface of a Homopolymer Layer. *Macromolecules* **1992**, *25*, 4967–4977.

20. Macosko, C. W.; Guégan, P.; Khandpur, A. K.; Nakayama, A.; Marechal, P.; Inoue, T. Compatibilizers for Melt Blending: Premade Block Copolymers†. *Macromolecules* **1996**, *29*, 5590–5598.

21. Bates, F. S.; Maurer, W. W.; Lipic, P. M.; Hillmyer, M. A.; Almdal, K.; Mortensen, K.; Fredrickson, G. H.; Lodge, T. P. Polymeric Bicontinuous Microemulsions. *Phys. Rev. Lett.* **1997**, *79*, 849.

22. Pernot, H.; Baumert, M.; Court, F.; Leibler, L. Design and Properties of Co-continuous Nanostructured Polymers by Reactive Blending. *Nat. Mater.* **2002**, *1*, 54–58.

23. Hillmyer, M. A.; Maurer, W. W.; Lodge, T. P.; Bates, F. S.; Almdal, K. Model Bicontinuous Microemulsions in Ternary Homopolymer Block Hopolymer Blends. *J. Phys. Chem. B* **1999**, *103*, 4814–4824.

24. Fredrickson, G. H.; Bates, F. S. Stabilizing Co-continuous Polymer Blend Morphologies with ABC Block Copolymers. *Eur. Phys. J. B* **1998**, *1*, 71–76.

25. Williams, J. M.; Gray, A. J.; Wilkerson, M. H. Emulsion Stability and Rigid Foams from Styrene or Divinylbenzene Water-in-Oil Emulsions. *Langmuir* **1990**, *6*, 437–444.

26. Kim, B. S.; Chiba, T.; Inoue, T. Morphology Development *via* Reaction-Induced Phase-Separation in Epoxy Poly(Ether Sulfone) Blends - Morphology Control Using Poly(Ether Sulfone) with Functional End-Groups. *Polymer* **1995**, *36*, 43–47.

27. Kim, B. J.; Kang, H. M.; Char, K.; Katsov, K.; Fredrickson, G. H.; Kramer, E. J. Interfacial Roughening Induced by the Reaction of End-Functionalized Polymers at a PS/P2VP Interface: Quantitative Analysis by DSIMS. *Macromolecules* **2005**, *38*, 6106–6114.

28. Binks, B. P. Particles as Surfactants - Similarities and Differences. *Curr. Opin. Colloid Interface Sci.* **2002**, *7*, 21–41.

29. Borrell, M.; Leal, L. G. Interfacial Activity of Polymer-Coated Gold Nanoparticles. *Langmuir* **2007**, *23*, 12497–12502.

30. Horozov, T. S.; Binks, B. P. Particle-Stabilized Emulsions: A Bilayer or a Bridging Monolayer? *Angew Chem., Int. Ed.* **2006**, *45*, 773–776.

31. Colver, P. J.; Colard, C. A. L.; Bon, S. A. F. Multilayered Nanocomposite Polymer Colloids Using Emulsion Polymerization Stabilized by Solid Particles. *J. Am. Chem. Soc.* **2008**, *130*, 16850–16851.

32. Menner, A.; Ikem, V.; Salgueiro, M.; Shaffer, M. S. P.; Bismarck, A. High Internal Phase Emulsion Templates Solely Stabilised by Functionalised Titania Nanoparticles. *Chem. Commun.* **2007**, 4274–4276.

33. Ikem, V. O.; Menner, A.; Bismarck, A. High Internal Phase Emulsions Stabilized Solely by Functionalized Silica Particles. *Angew. Chem.* **2008**, *120*, 8401–8403.

34. Chung, H.; Ohno, K.; Fukuda, T.; Composto, R. J. Self-Regulated Structures in Nanocomposites by Directed Nanoparticle Assembly. *Nano Lett.* **2005**, *5*, 1878–1882.

35. Chen, T.; Colver, P. J.; Bon, S. A. F. Organic-Inorganic Hybrid Hollow Spberes Prepared from TiO₂-Stabilized Pickering Emulsion Polymerization. *Adv. Mater.* **2007**, *19*, 2286–2289.

36. Li, C.; Han, J.; Ryu, C. Y.; Benicewicz, B. C. A Versatile Method To Prepare RAFT Agent Anchored Substrates and the Preparation of PMMA Grafted Nanoparticles. *Macromolecules* **2006**, *39*, 3175–3183.

37. Bockstaller, M. R.; Lapetnikov, Y.; Margel, S.; Thomas, E. L. Size-Selective Organization of Enthalpic Compatibilized Nanocrystals in Ternary Block Copolymer/Particle Mixtures. *J. Am. Chem. Soc.* **2003**, *125*, 5276–5277.

38. He, J. B.; Tangirala, R.; Emrick, T.; Russell, T. P.; Boker, A.; Li, X. F.; Wang, J. Self-Assembly of Nanoparticle-Copolymer Mixtures: A Kinetic Point of View. *Adv. Mater.* **2007**, *19*, 381–385.

39. Lin, Y.; Boker, A.; He, J. B.; Sill, K.; Xiang, H. Q.; Abetz, C.; Li, X. F.; Wang, J.; Emrick, T.; Long, S.; *et al.* Self-Directed Self-Assembly of Nanoparticle/Copolymer Mixtures. *Nature* **2005**, *434*, 55–59.

40. Zhao, Y.; Thorkelsson, K.; Mastroianni, A. J.; Schilling, T.; Luther, J. M.; Rancatore, B. J.; Matsunaga, K.; Jinnai, H.; Wu, Y.; Poulsen, D.; *et al.* Small-Molecule-Directed Nanoparticle Assembly Towards Stimuli-Responsive Nanocomposites. *Nat. Mater.* **2009**, *8*, 979–985.

41. Listak, J.; Bockstaller, M. R. Stabilization of Grain Boundary Morphologies in Lamellar Block Copolymer/Nanoparticle Blends. *Macromolecules* **2006**, *39*, 5820–5825.

42. Spontak, R. J.; Shankar, R.; Bowman, M. K.; Krishnan, A. S.; Hamersky, M. W.; Samseth, J.; Bockstaller, M. R.; Rasmussen, K. O. Selectivity- and Size-Induced Segregation of Molecular and Nanoscale Species in Microphase-Ordered Triblock Copolymers. *Nano Lett.* **2006**, *6*, 2115–2120.

43. Chen, X. C.; Green, P. F. Structure of Thin Film Polymer/Nanoparticle Systems: Polystyrene (PS) Coated-Au Nanoparticle/Tetramethyl Bisphenol-A Polycarbonate Mixtures (TMPC). *Soft Matter* **2011**, *7*, 1192–1198.

44. Kim, B. J.; Bang, J.; Hawker, C. J.; Kramer, E. J. Effect of Areal Chain Density on the Location of Polymer-Modified Gold Nanoparticles in a Block Copolymer Template. *Macromolecules* **2006**, *39*, 4108–4114.

45. Kim, B. J.; Chiu, J. J.; Yi, G. R.; Pine, D. J.; Kramer, E. J. Nanoparticle-Induced Phase Transitions in Diblock-Copolymer Films. *Adv. Mater.* **2005**, *17*, 2618–2622.

46. Chiu, J. J.; Kim, B. J.; Kramer, E. J.; Pine, D. J. Control of Nanoparticle Location in Block Copolymers. *J. Am. Chem. Soc.* **2005**, *127*, 5036–5037.

47. Kim, B. J.; Bang, J.; Hawker, C. J.; Chiu, J. J.; Pine, D. J.; Jang, S. G.; Yang, S. M.; Kramer, E. J. Creating Surfactant Nanoparticles for Block Copolymer Composites through Surface Chemistry. *Langmuir* **2007**, *23*, 12693–12703.

48. Tsutsumi, K.; Funaki, Y.; Hirokawa, Y.; Hashimoto, T. Selective Incorporation of Palladium Nanoparticles into Microphase-Separated Domains of Poly(2-vinylpyridine)-Block-Polyisoprene. *Langmuir* **1999**, *15*, 5200–5203.

49. Jang, S. G.; Khan, A.; Dimitriou, M. D.; Kim, B. J.; Lynd, N. A.; Kramer, E. J.; Hawker, C. J. Synthesis of Thermally Stable Au-Core/Pt-Shell Nanoparticles and Their Segregation Behavior in Diblock Copolymer Mixtures. *Soft Matter* **2011**, *7*, 6255–6263.

50. Cates, M. E.; Clegg, P. S.; Bijels, A New Class of Soft Materials. *Soft Matter* **2008**, *4*, 2132–2138.

51. Li, L.; Miesch, C.; Sudeep, P. K.; Balazs, A. C.; Emrick, T.; Russell, T. P.; Hayward, R. C. Kinetically Trapped Co-continuous Polymer Morphologies through Intraphase Gelation of Nanoparticles. *Nano Lett.* **2011**, *11*, 1997–2003.

52. Yoo, M.; Kim, S.; Lim, J.; Kramer, E. J.; Hawker, C. J.; Kim, B. J.; Bang, J. Facile Synthesis of Thermally Stable Core-Shell Gold Nanoparticles *via* Photo-Cross-Linkable Polymeric Ligands. *Macromolecules* **2010**, *43*, 3570–3575.

53. Kim, B. J.; Fredrickson, G. H.; Bang, J.; Hawker, C. J.; Kramer, E. J. Tailoring Core-Shell Polymer-Coated Nanoparticles as Block Copolymer Surfactants. *Macromolecules* **2009**, *42*, 6193–6201.

54. Kim, B. J.; Fredrickson, G. H.; Hawker, C. J.; Kramer, E. J. Nanoparticle Surfactants as a Route to Bicontinuous Block Copolymer Morphologies. *Langmuir* **2007**, *23*, 7804–7809.

55. Sacanna, S.; Kegel, W. K.; Philipse, A. P. Thermodynamically Stable Pickering Emulsions. *Phys. Rev. Lett.* **2007**, *98*, 158301.

56. Kim, B. J.; Fredrickson, G. H.; Kramer, E. J. Effect of Polymer Ligand Molecular Weight on Polymer-Coated Nanoparticle Location in Block Copolymers. *Macromolecules* **2008**, *41*, 436–447.

57. Mezzenga, R.; Ruokolainen, J.; Fredrickson, G. H.; Kramer, E. J. High Internal Phase Polymeric Emulsions by Self-Assembly of Colloidal Systems. *Macromolecules* **2003**, *36*, 4466–4471.

58. Keddie, J. L.; Meredith, P.; Jones, R. A. L; Donald, A. M. Film Formation of Acrylic Latices with Varying Concentrations of Non-Film-Forming Latex Particles. *Langmuir* **1996**, *12*, 3793–3801.

59. Mezzenga, R.; Ruokolainen, J.; Hexemer, A. On the Role of Block Copolymers in Self-Assembly of Dense Colloidal Polymeric Systems. *Langmuir* **2003**, *19*, 8144–8147.

60. Chen, T.; Colver, P. J.; Bon, S. A. F. Organic–Inorganic Hybrid Hollow Spheres Prepared from TiO$_2$-Stabilized Pickering Emulsion Polymerization. *Adv. Mater.* **2007**, *19*, 2286–2289.

61. Pieranski, P. Two-Dimensional Interfacial Colloidal Crystals. *Phys. Rev. Lett.* **1980**, *45*, 569–572.

62. Folkers, J. P.; Laibinis, P. E.; Whitesides, G. M. Self-Assembled Monolayers of Alkanethiols on Gold: Comparisons of Monolayers Containing Mixtures of Short- and Long-Chain Constituents with Methyl and Hydroxymethyl Terminal Groups. *Langmuir* **1992**, *8*, 1330–1341.

63. Shan, J.; Nuopponen, M.; Jiang, H.; Viitala, T.; Kauppinen, E.; Kontturi, K.; Tenhu, H. Amphiphilic Gold Nanoparticles Grafted with Poly(N-isopropylacrylamide) and Polystyrene. *Macromolecules* **2005**, *38*, 2918–2926.

64. Cho, J.-S.; Uchida, K.; Yoshioka, N.; Yamamoto, K. Electrical and Magnetic Properties of Electro-Oxidative Polymerized Poly(tris(thienylphenyl)amine)s. *Sci. Technol. Adv. Mater.* **2004**, *5*, 697–701.

65. Yeh, K.-M.; Lee, C.-C.; Chen, Y. Poly(4-vinyltriphenylamine): Optical, Electrochemical Properties and Its New Application as a Host Material of Green Phosphorescent Ir(ppy)3 Dopant. *Synth. Met.* **2008**, *158*, 565–571.

66. Choi, J.; Kwak, S. Y.; Kang, S.; Lee, S. S.; Park, M.; Lim, S.; Kim, J.; Choe, C. R.; Hong, S. I. Synthesis of Highly Crosslinked Monodisperse Polymer Particles: Effect of Reaction Parameters on the Size and Size Distribution. *J. Polym. Sci. A: Polym. Chem.* **2002**, *40*, 4368–4377.

67. Lim, J.; Yang, H.; Paek, K.; Cho, C.-H.; Kim, S.; Bang, J.; Kim, B. J. Click" Synthesis of Thermally Stable Au Nanoparticles with Highly Grafted Polymer Shell and Control of Their Behavior in Polymer Matrix. *J. Polym. Sci. A: Polym. Chem.* **2011**, *49*, 3464–3474.

68. Kwon, T.; Min, M.; Lee, H.; Kim, B. J. Facile Preparation of Water Soluble CuPt Nanorods with Controlled Aspect Ratio and Study on Their Catalytic Properties in Water. *J. Mater. Chem.* **2011**, *21*, 11956–11960.

69. Bai, L.; Ma, X.; Liu, J.; Sun, X.; Zhao, D.; Evans, D. G. Rapid Separation and Purification of Nanoparticles in Organic Density Gradients. *J. Am. Chem. Soc.* **2010**, *132*, 2333–2337.